

RSEA-MVGNN: Multi-View Graph Neural Network with Reliable Structural Enhancement and Aggregation

Junyu Chen¹, Long Shi¹, Badong Chen²

¹Financial Intelligence and Financial Engineering Key Laboratory of Sichuan Province, School of Computing and Artificial Intelligence, Southwestern University of Finance and Economics

²Institute of Artificial Intelligence and Robotics, Xi'an Jiaotong University
223081200039@smail.swufe.edu.cn, shilong@swufe.edu.cn, chenbd@mail.xjtu.edu.cn

Abstract

Graph Neural Networks (GNNs) have exhibited remarkable efficacy in learning from multi-view graph data. In the framework of multi-view graph neural networks, a critical challenge lies in effectively combining diverse views, where each view has distinct graph structure features (GSFs). Existing approaches to this challenge primarily focus on two aspects: 1) prioritizing the most important GSFs, 2) utilizing GNNs for feature aggregation. However, prioritizing the most important GSFs can lead to limited feature diversity, and existing GNN-based aggregation strategies equally treat each view without considering view quality. To address these issues, we propose a novel Multi-View Graph Neural Network with Reliable Structural Enhancement and Aggregation (RSEA-MVGNN). Firstly, we estimate view-specific uncertainty employing subjective logic. Based on this uncertainty, we design reliable structural enhancement by feature de-correlation algorithm. This approach enables each enhancement to focus on different GSFs, thereby achieving diverse feature representation in the enhanced structure. Secondly, the model learns view-specific beliefs and uncertainty as opinions, which are utilized to evaluate view quality. Based on these opinions, the model enables high-quality views to dominate GNN aggregation, thereby facilitating representation learning. Experimental results conducted on five real-world datasets demonstrate that RSEA-MVGNN outperforms several state-of-the-art GNN-based methods.

Introduction

Graphs are extensively employed for constructing and interpreting data that encompasses intricate interconnections. For example, in urban transportation networks (Sun et al. 2022), data is naturally depicted as a graph, with nodes symbolizing urban transportation stations and edges denoting the flow of traffic between nodes. In the analysis of traffic flow, each urban transportation station can collect data from different temporal scales, such as weekdays, weekends and monthly periods. This indicates that each node could be associated with multiple data sources. These characteristics spawn the emergence of an advanced graph modelling method, namely multi-view graph, which contains consistent nodes but shows different structures in each view. Multi-view graph representation learning (Hassani and Khasah-

Copyright © 2025, Association for the Advancement of Artificial Intelligence (www.aaai.org). All rights reserved.

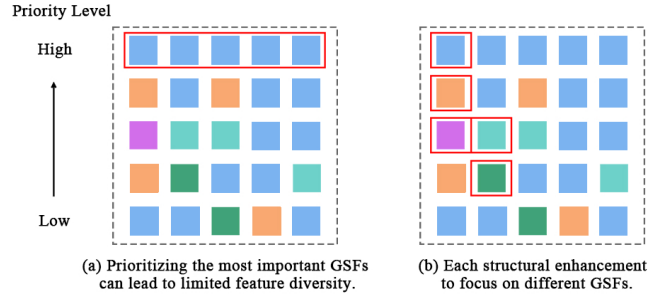


Figure 1: Visualization of the GSFs selected during structure enhancement. Squares of different colors represent nodes with different features in graphs. The red outlines indicate the enhanced nodes.

madi 2020; Zhang et al. 2021; Cheng et al. 2021) aims to merge information from various views into a compact, high quality representation. This area is garnering increasing research interest, and has found extensive applications in traffic analysis (Dai et al. 2023), disease diagnosis (Ramanathan and Martel 2023), protein prediction (Yan et al. 2020), and among others.

Early multi-view graph neural networks (MVGNNs) directly utilize GNNs for multi-view aggregation, such as Graph Convolutional Networks (GCNs) (Li, Li, and Wang 2020) and Graph Attention Networks (GATs) (Wang et al. 2019), focusing on the architectural design of MVGNNs to facilitate aggregation. Subsequently, MVGNNs evolve into more advanced frameworks (Liu et al. 2020a; Zhang et al. 2021; Zhao et al. 2023), which first prioritize view-specific graph structure features (GSFs) and then employ GNNs for aggregation. This approach enables MVGNNs to focus on important GSFs, thereby achieving more effective fusion.

In terms of GSFs processing, (Liu et al. 2020a) augments important features to construct latent graphs, (Zhao et al. 2023) selects the most crucial neighboring nodes to form an enhanced weight matrix, and (Yu et al. 2023) purifies key features to enrich separate views. Under this mechanism of prioritizing the most important GSFs, it inevitably leads to the result shown in Fig. 1 (a), namely limited feature diversity in the enhanced structure. Due to the fact of neglecting diverse GSFs information, this approach is unable to capture

a more comprehensive representation. In terms of aggregation, various types of GNN-based methods (Yao et al. 2022; Fu et al. 2020; Zhang et al. 2020) assume that different views have equal quality, thus all views participate equally in the aggregation process. This assumption is unreasonable, as the qualities of multiple views are different in practical scenes (Xu et al. 2024; Shi et al. 2024). Treating all views equally limits the positive contributions of high-quality views while allowing the negative impacts of low quality views on representation learning.

To address the above discussed issues, we propose the Multi-View Graph Neural Network with Reliable Structural Enhancement and Aggregation (RSEA-MVGNN). As illustration in Fig. 2, this framework includes two components: reliable structural enhancement and reliable aggregation. 1) Based on subjective logic theory (Sensoy, Kaplan, and Kandemir 2018; Han et al. 2022), we estimate view-specific uncertainty. The uncertainty reflects the degree of support provided by the view-specific predictions. To achieve reliable structural enhancement, we continue the enhancement process when uncertainty decreases after each iteration, and terminate it otherwise. The process employs a feature de-correlation algorithm for each enhancement. This approach enables focusing on different GSFs, thereby achieving diverse feature representation in the enhanced structure. 2) For reliable aggregation in MVGNN, we learn view-specific opinions consisting of belief masses and uncertainty. To evaluate view quality, we construct aggregation parameters based on these opinions. High-quality views have inclined category beliefs and lower uncertainty, resulting in larger aggregation parameters. Our model utilizes the parameters to enable high-quality views to dominate GNN aggregation, thereby achieving better multi-view graph representation learning.

Key contributions: 1) Reliable structural enhancement, utilizing uncertainty as a criterion to ensure more reliable enhancement results, and employing feature de-correlation to enrich the diversity of features in enhanced structures. 2) In the reliable aggregation, we utilize aggregation parameters to guide the fusion among multiple views. This approach enhances the positive contributions of high-quality views while limiting the negative impacts of low-quality views, thereby improving the performance of the multi-view graph aggregation. 3) The RSEA-MVGNN outperforms several state-of-the-art baselines. When compared to the existing top-performing method, it achieves a remarkable increase of 13.91% in the Ma-F1 score for classification tasks. Moreover, for clustering tasks, it obtains an improvement of 15.05% in the Adjusted Rand Index (ARI).

Related Work

Multi-View Graph Neural Networks: MVGNNs primarily focus on two crucial aspects: extracting GSFs and aggregating information from multi-view graphs. The extraction of GSFs determines the quality used in subsequent aggregation. Extracting GSFs has two main categories: Rule-based methods and adaptive methods. Rule-based methods (Liu et al. 2020c; Zhu et al. 2021; Bouritsas et al. 2022) rely on predefined rules or domain knowledge to extract GSFs.

These methods extract features based on graph topology, such as node degree (Lin et al. 2023) and centrality measures (Fang et al. 2023). Adaptive methods (Peng et al. 2021; Li et al. 2023) provide flexibility for enhancing critical GSFs. A typical example (Zhao et al. 2023) utilizes reinforcement learning to select the relevant neighborhoods. However, emphasizing the important GSFs may result in overlooking the diversity of GSFs and fail to capture a more comprehensive representation. Therefore, we design a reliable structural enhancement by feature de-correlation for ensuring diverse GSFs.

In terms of aggregation, MVGNNs primarily focus on neural network design. Specifically, GCN-based methods (Li, Li, and Wang 2020) unify GCNs and co-training into a single framework, enabling interaction fusion between views. GAT-based methods (Wang et al. 2019) employ hierarchical attention mechanisms that include node-level and semantic-level attentions. These methods treat all views equally, disregarding their different quality. However, each view has different quality in real-world scenarios. To tackle this limitation, we propose a reliable aggregation method based on view-specific opinions.

Uncertainty-based Deep Learning: In practice, a crucial challenge lies in handling varying quality of multimodal data (Zhang et al. 2024). To address this issue, uncertainty-based deep learning has emerged as a more general and principled approach for reliable multimodal fusion. Specifically, Evidential Deep Learning (EDL) (Sensoy, Kaplan, and Kandemir 2018) calculates category-specific evidence using a single deep neural network. Building on EDL, Trusted Multi-View Classification (Han et al. 2020) combines subjective logic and Dempster-Shafer theory to perform reliable fusion of multi-view. Furthermore, (Xu et al. 2024) introduced a conflictive opinion aggregation strategy and provided theoretical proof that uncertainty increases for conflictive instances. Similarly, quantifying uncertainty in GNNs has gained significant attention. (Wang et al. 2024) categorizes existing uncertainty quantification methods into single deterministic model (Stadler et al. 2021) and single model with random parameters (Cha, Kang, and Kang 2023). However, there is limited research exploring reliable aggregation in MVGNNs. Building on this observation, our research bridges the gap between multi-view uncertainty learning and GNN aggregation.

Our Method

This section begins with an introduction to MVGNNs and subjective logic preliminaries. Subsequently, we discuss the process of reliable structural enhancement and aggregation.

Preliminaries

Multi-view Graph Representation Learning. Let \mathcal{G} denote the collection of M distinct multi-view graphs, expressed as $\mathcal{G} = \{\mathcal{G}_i\}_{i=1}^M$. For any multi-view graph \mathcal{G}_i , it can be represented by $\mathcal{G}_i = \{\mathbf{G}_{i,j}\}_{j=1}^V$, where $\mathbf{G}_{i,j}$ denotes the graph corresponding to the j -th view within \mathcal{G}_i . In each graph $\mathbf{G}_{i,j} = \{N, E, \mathbf{A}, \mathbf{F}\}$, the set of nodes is $N = \{n_k\}_{k=1}^{|N|}$, and the set of edges is denoted by $E \subseteq$

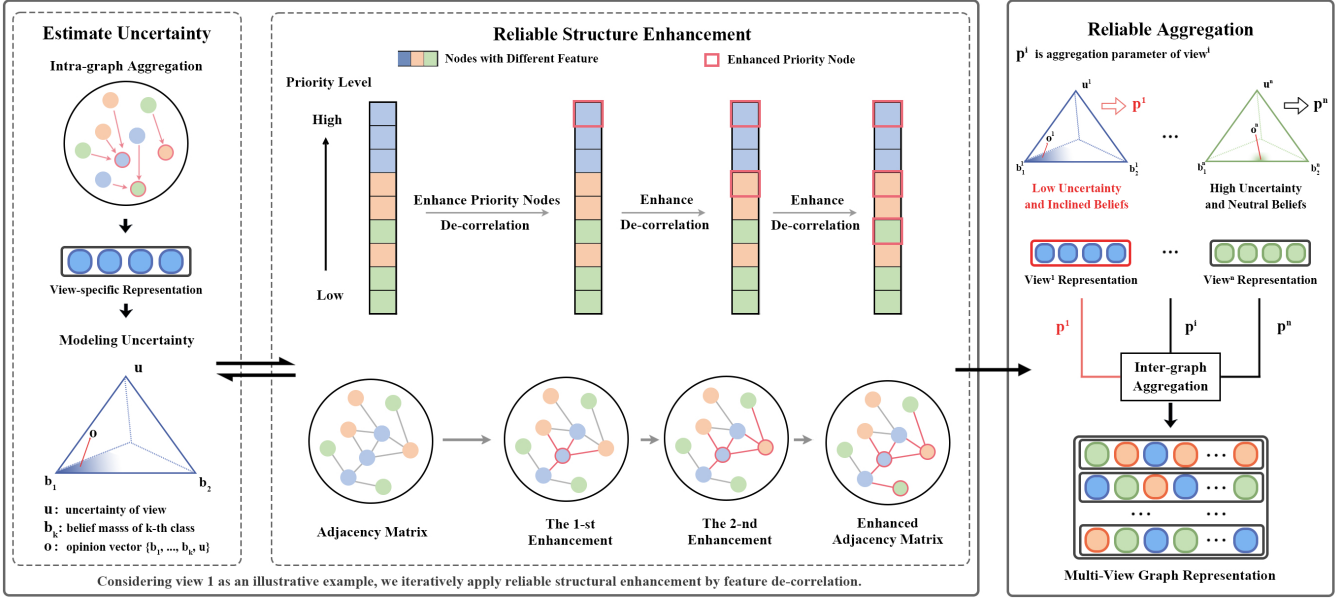


Figure 2: Illustration of RSEA-MVGNN. First, we learn view-specific beliefs and uncertainty as opinions. Based on the uncertainty, we apply reliable structural enhancement by feature de-correlation. Second, we construct aggregation parameters based on opinions of enhanced views, utilizing these parameters to facilitate high-quality views dominating inter-graph aggregation.

$N \times N$. The weighted adjacency matrix $\mathbf{A} \in \mathbb{R}^{|N| \times |N|}$, with $\mathbf{A}(k, k')$ quantifying the connection weight between node n_k and node $n_{k'}$. The feature matrix $\mathbf{F} \in \mathbb{R}^{|N| \times D}$, captures the node features across $|N|$ nodes and D dimensions, where $\mathbf{F}(k)$ represents the feature vector for node n_k . For multi-view graph representation learning, the objective is to embed the multi-view graphs $\mathcal{G} = \{\mathcal{G}_i\}_{i=1}^M$ into a low-dimensional and high quality feature matrix $\mathbf{Z} \in \mathbb{R}^{|M| \times D^{(l)}}$, where $D^{(l)}$ represents the dimension of feature at the l -th layer of representation learning process. Each \mathbf{Z}_i denotes the feature representation vector corresponding to a multi-view graph \mathcal{G}_i .

Multi-view Graph Neural Network. This GNN framework is tailored for learning representations of multi-view graphs. Given a multi-view graph \mathcal{G}_i , the j -th view is represented by $\mathbf{G}_{i,j}$, which includes an adjacency matrix $\mathbf{A}_{i,j}$ and a feature matrix $\mathbf{F}_{i,j}$. At the l -th layer for j -th view, the intra-graph feature fusion process is defined by the following equation:

$$\mathbf{F}_{i,j}^{(l*)} = \sigma \left(GNN_{intra}^{(l)} \left(\mathbf{F}_{i,j}^{(l-1)}, \mathbf{A}_{i,j}^{(l-1)} \right) \right), \quad (1)$$

where $\mathbf{F}_{i,j}^{(l*)}$ represents the intermediate feature matrix between the $(l-1)$ -th and l -th layer, $GNN_{intra}^{(l)}(\cdot)$ is the intra-graph fusion function at the l -th layer, and $\sigma(\cdot)$ denotes the activation function.

Subsequently, the inter-graph feature fusion process for the multi-view GNN at the l -th layer can be expressed as:

$$\mathbf{F}_{i,j}^{(l)} = \sigma \left(GNN_{inter}^{(l)} \left(\left\{ \mathbf{F}_{i,j}^{(l*)} \right\}_{j=1}^V \right) \right), \quad (2)$$

where $GNN_{inter}^{(l)}(\cdot)$ is the function for inter-graph fusion at the l -th layer, integrating graph features from different views.

Subjective Logic. Subjective logic provides a theoretical framework (Jsang 2018; Han et al. 2022) that associates the parameters of the Dirichlet distribution with the evidence from each view. This framework quantifies the overall uncertainty of the results from each view and reflects the reliability of the view.

The Dirichlet distribution is dependent on the parameters $\alpha = [\alpha_1, \dots, \alpha_K]$, which dictate the shape of the distribution. The Dirichlet Probability Density Function is defined as:

$$D(\mathbf{p}|\alpha) = \begin{cases} \frac{1}{B(\alpha)} \prod_{k=1}^K p_k^{\alpha_k-1}, & \text{for } \mathbf{p} \in S_K, \\ 0, & \text{otherwise,} \end{cases} \quad (3)$$

where the set S_K is the K -dimensional unit simplex, which defines the domain of the probability vector $\mathbf{p} = [p_1, \dots, p_K]^T$. Additionally, $B(\alpha)$ is the K -dimensional multinomial beta function.

In the subjective logic framework, for a given view $\mathbf{G}_{i,j}$, the evidence vector $\mathbf{e}_{i,j} = [e_1^{i,j}, \dots, e_K^{i,j}]$ is the classification result of a view-specific neural network. This vector $\mathbf{e}_{i,j}$ is applied to derive the belief vector $\mathbf{b}^{i,j} = [b_1^{i,j}, \dots, b_K^{i,j}]$, which reflects the reliability assigned to each of the K classes. Simultaneously, the uncertainty mass $u^{i,j}$ is the total uncertainty in the evidence vector. According to subjective logic, both $\mathbf{b}^{i,j}$ and $u^{i,j}$ are required to be non-negative, and

their sum must equal one:

$$\sum_{k=1}^K b_k^{i,j} + u^{i,j} = 1, \quad \forall k \in [1, \dots, K], \quad (4)$$

where $b_k^{i,j} \geq 0$ and $u^{i,j} \geq 0$.

In the j -th view, subjective logic associates the evidence $\mathbf{e}_{i,j}$, to the Dirichlet distribution parameters, $\boldsymbol{\alpha}_{i,j} = [\alpha_1^{i,j}, \dots, \alpha_K^{i,j}]$. Specifically, each $\alpha_k^{i,j}$ is calculated by $\alpha_k^{i,j} = e_k^{i,j} + 1$. Following this approach, the belief mass $b_k^{i,j}$ and the uncertainty $u^{i,j}$ are determined by the formulas:

$$b_k^{i,j} = \frac{e_k^{i,j}}{S^{i,j}} = \frac{\alpha_k^{i,j} - 1}{S^{i,j}} \quad \text{and} \quad u^{i,j} = \frac{K}{S^{i,j}}, \quad (5)$$

where $S^{i,j} = \sum_{k=1}^K (e_k^{i,j} + 1) = \sum_{k=1}^K \alpha_k^{i,j}$ is the Dirichlet strength. Consequently, by utilizing the Dirichlet distribution, subjective logic enables the modeling of both second-order probabilities and uncertainty in neural network outputs (Han et al. 2020).

Reliable Structural Enhancement and Aggregation

Estimate Uncertainty of Intra-GNN. To estimate the uncertainty in intra-graph feature fusion, we first employ a Graph Convolutional Network. This process is described by the following equation:

$$\mathbf{F}_{i,j}^{(l*)} = \sigma \left(\mathbf{A}_{i,j}^{(l-1)} \mathbf{F}_{i,j}^{(l-1)} \mathbf{W}_{intra,i,j}^{(l)} \right), \quad (6)$$

where $\mathbf{W}_{intra,i,j}^{(l)}$ is the weight matrix corresponding to the intra-graph fusion at l -th layer. Building on this, we utilize a single-layer feedforward neural network (FNN) to process the result of the intra-graph fusion. The FNN generates the evidence $\mathbf{e}_{i,j}$ for j -th view, specifically:

$$\mathbf{e}_{i,j} = \hat{\sigma} \left(\mathbf{F}_{i,j}^{(l*)} \mathbf{W}_{fnn,i,j}^{(l)} \right), \quad (7)$$

where $\mathbf{W}_{fnn,i,j}^{(l)}$ is the weight matrix of the FNN, $\hat{\sigma}$ refers to the softplus activation function. The softplus function is employed to ensure non-negative network output, which is necessary for acquiring the parameters of the Dirichlet distribution. In the subjective logic framework, following Eq. (5) from the preliminaries, the total uncertainty $u^{i,j}$ is calculated based on the evidence vector $\mathbf{e}_{i,j}$.

Reliable Structural Enhancement. Fig. 2 shows the process for reliable structural enhancement. To enhance structures with diverse features and reduce uncertainty, we apply reliable structural enhancement by feature de-correlation. This algorithm enables each structural enhancement to focus on different GSFs. Algorithm 1 is designed to enhance structure while performing feature de-correlation. Specifically, for a graph $\mathbf{G}_{i,j}$, we apply degree centrality to its adjacency matrix $\mathbf{A}_{i,j}$ to measure the influence of nodes in the graph. Concurrently, we analyze the variance of node features in the matrix $\mathbf{F}_{i,j}$, quantifying the diverse feature information exhibited by the nodes. For k -th node, the node priority level is calculated by:

$$\phi_k = CEN(\mathbf{A}_{i,j}(k)) + VAR(\mathbf{F}_{i,j}(k)), \quad (8)$$

Algorithm 1: Reliable Structural Enhancement by Feature De-correlation

Input: The adjacency matrix $\mathbf{A}_{i,j}$, the feature matrix $\mathbf{F}_{i,j}$

Output: The enhanced adjacency matrix $\hat{\mathbf{A}}_{i,j}$

- 1: Initialize uncertainty $U = \infty$
 - 2: Initialize enhancement number $R = 0$
 - 3: Iteration factor $T = 0.05|N|$
 - 4: Calculate degree centrality vector $\boldsymbol{\Delta} = [\delta_1, \dots, \delta_{|N|}]$ based on the adjacency matrix $\mathbf{A}_{i,j}$, where δ_i is the degree centrality of the i -th node
 - 5: Calculate variance vector $\boldsymbol{\Theta} = [\theta_1, \dots, \theta_{|N|}]$ based on the feature matrix $\mathbf{F}_{i,j}$, where θ_i is the variance of features for the i -th node
 - 6: Calculate the priority level vector $\boldsymbol{\Phi} = \boldsymbol{\Delta} + \boldsymbol{\Theta}$
 - 7: **while** $True$ **do**
 - 8: Intermediate feature $\mathcal{F}^{(l*)}(:, j, :, :)$ by Eq. (6)
 - 9: Uncertainty U' by Eq. (5) and (7)
 - 10: **if** $U' \leq U$ **then**
 - 11: Update uncertainty $U = U'$
 - 12: Update enhancement number $R = R + T$
 - 13: **for** $iter = 1$ to R **do**
 - 14: Find the priority index $Ind = \arg \max_k \phi_k$
 - 15: Enhance the priority Ind -th node by Eq. (9)
 - 16: Update $\boldsymbol{\Phi}$ by applying the feature de-correlation process according to Eq. (10)
 - 17: **end for**
 - 18: **else**
 - 19: $Break$
 - 20: **end if**
 - 21: **end while**
-

where $\mathbf{A}_{i,j}(k)$ and $\mathbf{F}_{i,j}(k)$, represent the adjacency vector and feature vector of k -th node. The degree centrality and variance are calculated using $CEN(\cdot)$ and $VAR(\cdot)$, respectively. The priority level vector $\boldsymbol{\Phi} = [\phi_1, \dots, \phi_{|N|}]$ represents the importance of nodes in the view $\mathbf{G}_{i,j}$, where higher values indicate higher priority.

The node with the highest value in $\boldsymbol{\Phi}$ is selected as the priority node, denoted as the Ind -th node. We obtain the priority adjacency vector $\mathbf{A}_{i,j}(Ind)$, where each positive weight represents an effective connection to other nodes. To construct the adjacency vector mask for the Ind -th node, denoted by $\tilde{\mathbf{A}}_{i,j}(Ind)$, we assign one to each positive weight in $\mathbf{A}_{i,j}(Ind)$, and zero to all others. The priority adjacency vector $\mathbf{A}_{i,j}(Ind)$ is enhanced by the following equation:

$$\hat{\mathbf{A}}_{i,j}(Ind) = \max(\mathbf{A}_{i,j}) \tilde{\mathbf{A}}_{i,j}(Ind), \quad (9)$$

where $\max(\mathbf{A}_{i,j})$ serves to select the maximum edge weight in the adjacency matrix $\mathbf{A}_{i,j}$. The enhanced adjacency vector $\hat{\mathbf{A}}_{i,j}(Ind)$ means the edges with positive weights of the Ind -th node are enhanced to $\max(\mathbf{A}_{i,j})$. By enhancing the edge weights of the Ind -th node, we increase its connectivity within the network, thereby improving its influence in the propagation process of the GNN.

To ensure diversity in subsequently enhanced priority nodes, we reduce the priority level of nodes with similar fea-

tures. The priority level of ϕ_k is updated by:

$$\phi_k = \phi_k(1 - \text{COS}(\mathbf{F}_{i,j}(k), \mathbf{F}_{i,j}(\text{Ind}))) \quad (10)$$

where $\text{COS}(\cdot)$ measures the cosine similarity between the node feature vectors $\mathbf{F}_{i,j}(k)$ and $\mathbf{F}_{i,j}(\text{Ind})$. The priority level vector Φ is updated for each node by Eq. (10).

Following Algorithm 1, we alternately estimate uncertainty and enhance structure through feature de-correlation. If uncertainty decreases after each enhancement, we increase the number of enhanced nodes for the next enhancement. We continue the enhancement process when uncertainty decreases after each iteration, and terminate it otherwise. After reliable structural enhancement, we obtain the enhanced adjacency matrix $\hat{\mathbf{A}}_{i,j}$, which exhibits lower uncertainty and greater diversity in features representation.

Reliable Aggregation. To achieve reliable aggregation, we measure view-specific opinions consisting of belief vector $\mathbf{b}^{i,j}$ and uncertainty mass $u^{i,j}$. Based on opinions, we construct the aggregation parameter to evaluate view quality. The aggregation parameter $p_{i,j}$ is calculated by:

$$p_{i,j} = \text{VAR}(\mathbf{b}^{i,j})/u^{i,j} \quad (11)$$

where variance is calculated using $\text{VAR}(\cdot)$. High-quality views have inclined category beliefs and lower uncertainty, resulting in larger aggregation parameters. For example, under a triple classification task, given $\mathbf{b}^{i,0} = [0.4, 0.1, 0.1]$ and $\mathbf{b}^{i,1} = [0.2, 0.2, 0.2]$, the $\mathbf{b}^{i,0}$ have larger variance and more inclined category beliefs, which reveal more meaningful insights. The uncertainty $u^{i,j}$ is inverted to represent reliability and serves as the denominator. Our model utilizes the aggregation parameters to enable high-quality views to dominate the inter-graph aggregation.

In the inter-graph feature aggregation process, we guide reliable aggregation by utilizing the aggregation parameter vector $\mathbf{p}_i = [p_{i,1}, \dots, p_{i,V}]$. To align with the dimensions of intermediate feature tensor $\text{TRAN}_{1,2}(\mathcal{F}_i^{(l*)})$, we span \mathbf{p}_i and denote the result as \mathcal{P}_i . Here, \mathcal{P}_i represents the quality of multiple views. We define the inter-graph reliable aggregation process:

$$\text{TRAN}_{1,2}(\mathcal{F}_i^{(l)}) = \sigma(\mathcal{P}_i \odot \text{TRAN}_{1,2}(\mathcal{F}_i^{(l*)}) \mathcal{W}_{inter,i}^{(l)}), \quad (12)$$

where $\mathcal{W}_{inter,i}^{(l)}$ is the weight tensor for the inter-graph aggregation of i -th view in l -th layer, and operation \odot denotes the Hadamard product. Based on \mathcal{P}_i , each view is participates in the inter-graph aggregation according to its quality. Consequently, views with higher quality have a greater influence on the inter-graph aggregation process. Our research bridges the gap between multi-view uncertainty learning and GNN aggregation. The reliable aggregation method differentially treats views of varying quality. This novel approach enhances the positive contribution of reliable views while mitigating the impact of less reliable ones, achieving reliable multi-view graph aggregation.

In the final layer, we vectorize $\mathcal{F}_i^{(l)}$ to obtain the result of our multi-view graph representation learning, represented

by $\mathbf{Z}_i \in \mathbb{R}^{1 \times D^{(l)}}$. This process is implemented using mean pooling:

$$\mathbf{z}_i = \frac{1}{V|N|} \sum_{j=1}^V \sum_{k=1}^{|N|} \mathcal{F}^{(l)}(i, j, k, :), \quad (13)$$

where \mathbf{Z}_i denotes the i -th row of the feature representation matrix \mathbf{Z} , corresponding to the i -th multi-view graph instance \mathcal{G}_i .

Optimization

In the design of the loss function, based on the theory of subjective logic, we obtain the parameter α and form the Dirichlet Probability Density Function $D(\mathbf{p}|\alpha)$, where \mathbf{p} is the class assignment probabilities on a simplex. We formulate the adjusted cross-entropy loss function (Han et al. 2022):

$$\begin{aligned} \mathcal{L}_{ace}(\alpha) &= \int \left[\sum_{k=1}^K -Y_k \log(p_k) \right] \frac{\prod_{k=1}^K p_k^{\alpha_k - 1}}{B(\alpha)} d\mathbf{p} \\ &= \sum_{k=1}^K Y_k (\psi(S) - \psi(\alpha_k)), \end{aligned} \quad (14)$$

where Y_k is the actual label and p_k is the predicted probability for the k -th class. The strength S of Dirichlet distribution is given by Eq. (5), and the term $\psi(\cdot)$ is defined as the digamma function. Eq. (14) represents the integral of the cross-entropy loss function over the simplex defined by α .

The overall loss of RSEA-MVGNN is defined as follows:

$$\mathcal{L}_{all} = \sum_{l=1}^L \left[\mathcal{L}_{ace}(\alpha^{(l)}) + \sum_{j=1}^V \mathcal{L}_{ace}(\alpha_j^{(l)}) + \lambda \|\Theta^{(l)}\|_2 \right], \quad (15)$$

where $\alpha_j^{(l)}$ and $\alpha^{(l)}$ are respectively constructed from the evidence formulated by Eqs. (6) and (12). To mitigate the risk of overfitting, we introduce a regularization term $\Theta^{(l)}$, with λ serving as the regularization coefficient.

Experiments

In this section, we conduct comprehensive experiments to evaluate the performance of the proposed RSEA-MVGNN on five domain-specific datasets. Our evaluation includes a diverse set of tasks including classification, clustering, ablation studies, computational complexity analysis. More details are shown in the appendix.

Dataset	Instances	Classes	Features	Views
HIV	70	2	90	fMRI&DTI
BikeDC	72	4	267	weekday&weekend&month
PROTEINS	1000	2	80	sequence&molecule interaction
ogbg-molhiv	41127	2	9	self-duplicate
ACM	3025	3	1830	APA&APSPA

Table 1: Datasets Statistics

Table 2: Experimental results (%) for classification and clustering tasks on datasets.

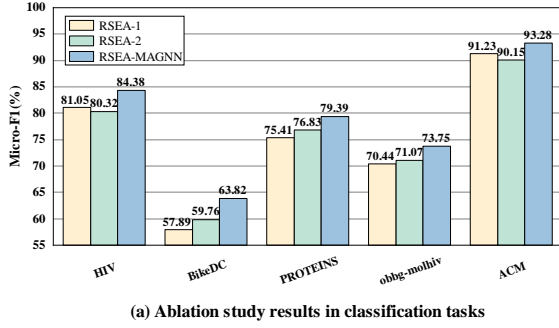
Datasets	Metrics Train%	Ma-F1		Mi-F1		NMI	ARI
		20%	60%	20%	60%		
HIV	HAN	58.90 ± 5.04	69.55 ± 4.23	60.00 ± 3.64	70.62 ± 4.88	23.73 ± 7.17	17.59 ± 14.75
	MAGNN	56.66 ± 4.75	69.84 ± 4.59	58.43 ± 3.14	71.25 ± 5.00	19.30 ± 10.96	20.33 ± 11.98
	TensorGCN	59.02 ± 4.38	70.98 ± 4.36	60.31 ± 2.81	72.50 ± 5.00	24.38 ± 13.50	19.44 ± 9.14
	RTGNN	65.74 ± 5.75	75.14 ± 8.18	67.50 ± 6.43	76.25 ± 08.29	35.02 ± 11.43	30.86 ± 10.81
	PTGB	68.33 ± 6.78	81.74 ± 8.12	70.24 ± 8.04	82.57 ± 8.43	36.24 ± 9.35	34.78 ± 9.49
	AdaSNN	62.56 ± 6.37	72.48 ± 6.96	63.88 ± 6.47	73.22 ± 6.84	34.57 ± 8.61	34.67 ± 9.01
	RSEF-MVGNN	70.58 ± 3.82	83.43 ± 5.38	72.34 ± 3.01	84.38 ± 5.03	49.31 ± 15.92	49.83 ± 22.40
	Gain	2.25	1.69	2.10	1.81	13.07	15.05
BikeDC	HAN	25.40 ± 2.26	33.07 ± 5.16	40.00 ± 3.52	50.00 ± 3.94	49.58 ± 8.66	31.41 ± 9.42
	MAGNN	24.04 ± 3.53	32.10 ± 6.47	37.05 ± 4.20	49.41 ± 6.55	50.74 ± 7.35	29.74 ± 8.61
	TensorGCN	25.30 ± 2.68	33.99 ± 8.56	40.29 ± 3.73	50.58 ± 9.18	51.22 ± 7.08	31.47 ± 8.07
	RTGNN	35.22 ± 7.25	48.25 ± 5.10	45.88 ± 3.76	57.05 ± 4.59	52.13 ± 7.97	31.40 ± 8.55
	PTGB	26.68 ± 9.45	35.73 ± 9.22	27.31 ± 9.32	36.35 ± 9.61	50.64 ± 7.54	31.48 ± 7.17
	AdaSNN	30.49 ± 7.14	40.73 ± 7.27	31.80 ± 7.33	41.42 ± 7.56	53.48 ± 6.68	31.02 ± 6.84
	RSEF-MVGNN	48.23 ± 6.80	62.16 ± 8.74	51.47 ± 5.46	63.82 ± 8.58	55.57 ± 6.85	32.35 ± 6.72
	Gain	13.04	13.91	5.59	6.77	2.09	0.87
PROTEINS	HAN	71.98 ± 0.59	76.04 ± 0.51	72.58 ± 0.62	76.83 ± 0.50	12.86 ± 2.48	14.43 ± 3.64
	MAGNN	72.19 ± 0.59	75.97 ± 1.25	72.66 ± 0.65	76.58 ± 1.24	13.12 ± 2.97	15.78 ± 2.86
	TensorGCN	72.19 ± 0.60	75.93 ± 0.69	72.75 ± 0.58	76.50 ± 0.67	12.98 ± 3.43	17.34 ± 3.12
	RTGNN	73.28 ± 0.48	77.08 ± 1.18	73.81 ± 0.54	77.79 ± 1.19	14.77 ± 2.71	21.39 ± 2.56
	PTGB	65.37 ± 5.23	68.32 ± 4.67	66.14 ± 4.81	69.82 ± 4.65	15.84 ± 4.30	17.28 ± 4.27
	AdaSNN	73.68 ± 1.28	77.16 ± 1.03	73.22 ± 1.75	78.53 ± 1.86	19.53 ± 2.28	22.62 ± 3.48
	RSEF-MVGNN	73.94 ± 1.40	78.34 ± 1.89	73.93 ± 1.22	79.39 ± 1.67	21.07 ± 2.19	24.47 ± 2.87
	Gain	0.26	1.18	0.12	0.86	1.54	1.85
ogbg-molhiv	HAN	63.39 ± 2.66	65.28 ± 2.55	65.52 ± 2.87	66.92 ± 2.74	14.20 ± 5.77	14.74 ± 5.62
	MAGNN	64.84 ± 2.88	66.34 ± 2.80	66.52 ± 3.12	67.28 ± 2.96	15.03 ± 3.65	15.46 ± 3.23
	TensorGCN	65.43 ± 2.33	66.64 ± 2.55	68.15 ± 2.84	70.09 ± 2.98	14.81 ± 3.83	15.72 ± 4.11
	RTGNN	67.09 ± 4.61	68.17 ± 4.77	71.85 ± 5.10	72.33 ± 5.21	15.88 ± 3.44	17.58 ± 3.92
	PTGB	55.95 ± 3.34	58.40 ± 3.22	57.35 ± 3.15	59.03 ± 3.44	16.05 ± 4.84	16.49 ± 4.68
	AdaSNN	72.84 ± 4.45	74.93 ± 4.34	73.19 ± 4.28	75.55 ± 4.31	19.82 ± 3.95	21.47 ± 4.08
	RSEF-MVGNN	73.09 ± 3.14	75.53 ± 2.82	73.75 ± 3.11	76.08 ± 2.97	23.69 ± 4.55	26.77 ± 5.03
	Gain	0.25	0.60	0.56	0.53	3.87	5.30
ACM	HAN	91.06 ± 0.18	91.18 ± 0.24	91.11 ± 0.23	91.26 ± 0.36	61.56 ± 0.87	64.39 ± 0.95
	MAGNN	91.93 ± 0.25	92.17 ± 0.22	92.03 ± 0.22	92.34 ± 0.21	62.32 ± 1.06	64.77 ± 1.24
	TensorGCN	92.30 ± 0.33	92.49 ± 0.39	92.37 ± 0.35	92.52 ± 0.38	62.18 ± 1.13	64.05 ± 1.37
	RTGNN	92.68 ± 0.37	92.88 ± 0.41	92.75 ± 0.39	93.07 ± 0.46	62.79 ± 0.92	65.18 ± 0.83
	RSEF-MVGNN	93.19 ± 0.33	93.07 ± 0.35	93.28 ± 0.44	93.37 ± 0.42	64.15 ± 0.73	66.97 ± 0.84
	Gain	0.51	0.19	0.53	0.30	1.36	1.79

Experimental Settings

Dataset Details. 1) **Human Immunodeficiency Virus (HIV)** (Ragin et al. 2012) contains two types of imaging: functional magnetic resonance imaging (fMRI) and diffusion tensor imaging (DTI). Each instance includes DTI-derived brain graphs that share the same nodes with those derived from fMRI. 2) **Capital Bikeshare Data (BikeDC)** (Sun et al. 2022) is collected from the Washington D.C. Bicycle System. Each instance is characterized by three temporal views: weekday, weekend, and monthly traffic patterns, which capture the complex traffic dynamics across 267 aggregated stations. 3) **PROTEINS** (Borgwardt et al. 2005; Adaloglou, Vretos, and Daras 2020) includes 1,000 protein molecule instances. Each instance contains two views: the sequence view and the molecule interaction view. 4) **ogbg-molhiv** (Hu et al. 2020) derived from MoleculeNet. Each

instance in these datasets represents a molecule as a graph, where atoms are nodes and chemical bonds are edges. To address the scarcity of multi-view graph data for graph-level prediction tasks, we duplicate the original view to create a second view. 5) **ACM** (Wang et al. 2019) is derived from the ACM database, comprising two views: a co-paper graph (author-paper relationships) and a co-subject graph (subject-paper connections).

Compared Methods. 1) **HAN** (Wang et al. 2019) aggregates relation-specific features from various graphs using attention techniques. 2) **MAGNN** (Fu et al. 2020) learns node attributes through linear transformation and aggregates information at a specialized encoder. 3) **TensorGCN** (Liu et al. 2020b) is a tensor GCN-based representation learning method for multi-view graphs. 4) **RTGNN** (Zhao et al.



(a) Ablation study results in classification tasks

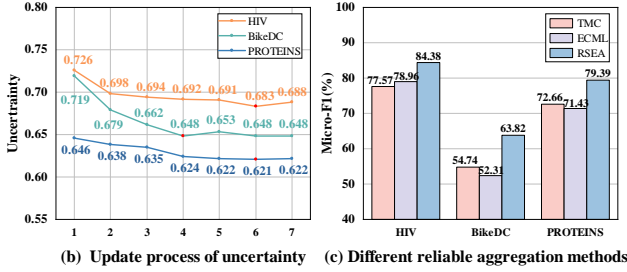


Figure 3: Ablation Study for RSEA-MVGNN.

2023) introduces a novel tensor GNN framework that enhances multi-view graph representation through reinforcement learning. 5) **PTGB** (Yang, Cui, and Yang 2023) proposes a GNN pretraining framework for brain networks that captures intrinsic brain network structures. 6) **AdaSNN** (Li et al. 2023) proposes an adaptive subgraph neural network to detect critical structures in graphs.

Implementation Details. Following the previous works (Zhao et al. 2023; Fu et al. 2020), we process the low-dimensional feature vectors generated by each method through Support Vector Machine (SVM) for classification tasks and through the K-means algorithm for clustering tasks. Specifically, for the SVM, we evaluate its performance across distinct training ratios, specifically at 20% and 60%, where the test set is provided to the linear SVM. In terms of clustering, the predefined number of classes in each multi-view dataset determines the number of clusters used in the K-means algorithm.

Overall Performance (RQ1)

Table 2 presents the performance comparison between RSEA-MVGNN and various baseline methods, with the best results highlighted in bold. Based on the results shown in Table 2, we draw the following conclusions: 1) RSEA-MVGNN achieves top-performing performance across all five datasets, improving classification by 13.91% (BikeDC) and clustering by 15.05% (HIV). 2) RSEA-MVGNN notably improves weaker results in both classification and clustering tasks. On the HIV dataset, while PTGB performs well in classification (82.57% Mi-F1), it shows poor results in clustering (34.67% ARI). RSEA-MVGNN significantly enhances the weaker clustering results, improving both NMI and ARI by over 13%. Similar improvements are

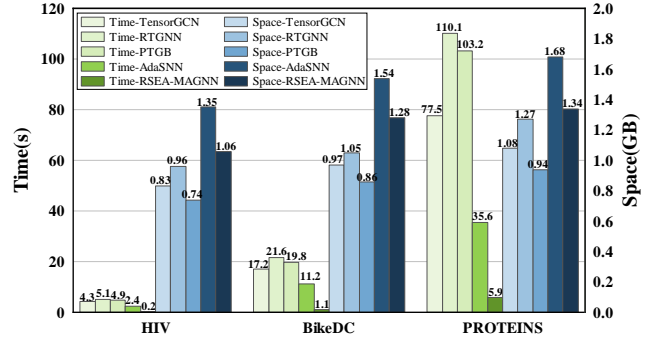


Figure 4: Execution Time (seconds) and Space Requirements (gigabytes).

seen in classification on BikeDC; clustering on PROTEINS, obbg-molhiv, and ACM datasets. 3) RSEA-MVGNN outperforms on five diverse datasets, while PTGB, a brain network-specific model, shows lower F1 scores on other domains. This highlights RSEA-MVGNN’s effective generalization without domain-specific expert knowledge.

Ablation Study (RQ2)

Fig. 3 (a) shows two RSEA-MAGNN variants: RSEA-1 lacks reliable structural enhancement, only enhancing a fixed number of priority nodes. RSEA-2 excludes the reliable aggregation in the inter-graph fusion. Neither variants of RSEA-MAGNN achieves the best performance. Fig. 3 (b) visualizes the uncertainty reduction process, showing varying degrees of decrease across datasets during structural enhancement. Fig. 3 (c) shows classification tests comparing RSEA-MAGNN with reliable methods TMC (Han et al. 2020) and ECML (Xu et al. 2024). The results demonstrate that RSEA-MAGNN has advantage, indicating the necessity of introducing reliable mechanisms into GNNs for processing graph-type data.

Computational Complexity Analysis (RQ3)

Fig. 4 compares execution time and memory usage of five methods on various datasets, tested on an NVIDIA RTX 4090 GPU. RSEA-MVGNN shows significantly shorter execution time with comparable memory requirements. The training process of RSEA-MVGNN including reliable structural enhancement with $\mathcal{O}(VMN^2)$, intra-graph aggregation with $\mathcal{O}(VN^2D)$, and inter-graph reliable aggregation with $\mathcal{O}(VNC^2)$. The overall time complexity can be represented as $\mathcal{O}(LVMN^2 + LVN^2D + LVNC^2)$, which simplifies to $\mathcal{O}(LVN^2(M + D))$.

Conclusion

In this paper, we propose a novel multi-view GNN-based framework for representation learning, termed as RSEA-MVGNN. To enhance the graph’s structural robustness and feature diversity, we design the reliable structural enhancement by feature de-correlation algorithm. For the purpose of

enabling reliable aggregation in multi-view GNNs, we construct aggregation parameters, enabling high-quality views to dominate the inter-graph aggregation process. These two modules can be easily adapted to various GNN architectures. Experimental results show RSEA-MVGNN outperforms state-of-the-art baselines in multi-view graph neural networks.

References

- Adaloglou, N.; Vretos, N.; and Daras, P. 2020. *Multi-view Adaptive Graph Convolutions for Graph Classification*, 398–414.
- Borgwardt, K. M.; Ong, C. S.; Schonauer, S.; Vishwanathan, S. V. N.; Smola, A. J.; and Kriegel, H.-P. 2005. Protein function prediction via graph kernels. *Bioinformatics*, i47–i56.
- Bouritsas, G.; Frasca, F.; Zafeiriou, S.; and Bronstein, M. M. 2022. Improving graph neural network expressivity via subgraph isomorphism counting. *IEEE Transactions on Pattern Analysis and Machine Intelligence*, 45(1): 657–668.
- Cha, S.; Kang, H.; and Kang, J. 2023. On the temperature of bayesian graph neural networks for conformal prediction. *arXiv preprint arXiv:2310.11479*.
- Cheng, J.; Wang, Q.; Tao, Z.; Xie, D.; and Gao, Q. 2021. Multi-view attribute graph convolution networks for clustering. In *Proceedings of the twenty-ninth international conference on international joint conferences on artificial intelligence*, 2973–2979.
- Dai, S.; Wang, J.; Huang, C.; Yu, Y.; and Dong, J. 2023. Dynamic Multi-View Graph Neural Networks for Citywide Traffic Inference. *ACM Trans. Knowl. Discov. Data*, 17(4).
- Fang, U.; Li, M.; Li, J.; Gao, L.; Jia, T.; and Zhang, Y. 2023. A comprehensive survey on multi-view clustering. *IEEE Transactions on Knowledge and Data Engineering*.
- Fu, X.; Zhang, J.; Meng, Z.; and King, I. 2020. MAGNN: Metapath Aggregated Graph Neural Network for Heterogeneous Graph Embedding. In *Proceedings of The Web Conference 2020*.
- Han, Z.; Zhang, C.; Fu, H.; and Zhou, J. T. 2020. Trusted multi-view classification. In *International Conference on Learning Representations*.
- Han, Z.; Zhang, C.; Fu, H.; and Zhou, J. T. 2022. Trusted multi-view classification with dynamic evidential fusion. *IEEE transactions on pattern analysis and machine intelligence*, 45(2): 2551–2566.
- Hassani, K.; and Khasahmadi, A. H. 2020. Contrastive multi-view representation learning on graphs. In *International conference on machine learning*, 4116–4126. PMLR.
- Hu, W.; Fey, M.; Zitnik, M.; Dong, Y.; Ren, H.; Liu, B.; Catasta, M.; and Leskovec, J. 2020. Open graph benchmark: Datasets for machine learning on graphs. *Advances in neural information processing systems*, 33: 22118–22133.
- Jsang, A. 2018. *Subjective Logic: A formalism for reasoning under uncertainty*. Springer Publishing Company, Incorporated.
- Li, J.; Sun, Q.; Peng, H.; Yang, B.; Wu, J.; and Phillip, S. Y. 2023. Adaptive subgraph neural network with reinforced critical structure mining. *IEEE Transactions on Pattern Analysis and Machine Intelligence*.
- Li, S.; Li, W.-T.; and Wang, W. 2020. Co-gcn for multi-view semi-supervised learning. In *Proceedings of the AAAI conference on artificial intelligence*, volume 34, 4691–4698.
- Lin, Z.; Kang, Z.; Zhang, L.; and Tian, L. 2023. Multi-View Attributed Graph Clustering. *IEEE Transactions on Knowledge and Data Engineering*, 35(2): 1872–1880.
- Liu, Q.; Kampffmeyer, M. C.; Jenssen, R.; and Salberg, A.-B. 2020a. Multi-view self-constructing graph convolutional networks with adaptive class weighting loss for semantic segmentation. In *Proceedings of the IEEE/CVF conference on computer vision and pattern recognition workshops*, 44–45.
- Liu, X.; You, X.; Zhang, X.; Wu, J.; and Lv, P. 2020b. Tensor Graph Convolutional Networks for Text Classification. *Proceedings of the AAAI Conference on Artificial Intelligence*, 8409–8416.
- Liu, Z.; Dou, Y.; Yu, P. S.; Deng, Y.; and Peng, H. 2020c. Alleviating the inconsistency problem of applying graph neural network to fraud detection. In *Proceedings of the 43rd international ACM SIGIR conference on research and development in information retrieval*, 1569–1572.
- Peng, H.; Zhang, R.; Dou, Y.; Yang, R.; Zhang, J.; and Yu, P. S. 2021. Reinforced neighborhood selection guided multi-relational graph neural networks. *ACM Transactions on Information Systems (TOIS)*, 40(4): 1–46.
- Ragin, A. B.; Du, H.; Ochs, R.; Wu, Y.; Sammet, C. L.; Shoukry, A.; and Epstein, L. G. 2012. Structural brain alterations can be detected early in HIV infection. *Neurology*, 79(24): 2328–2334.
- Ramanathan, V.; and Martel, A. L. 2023. Self Supervised Multi-view Graph Representation Learning in Digital Pathology. In *International Conference on Medical Image Computing and Computer-Assisted Intervention*, 74–84. Springer.
- Sensoy, M.; Kaplan, L.; and Kandemir, M. 2018. Evidential Deep Learning to Quantify Classification Uncertainty. *Neural Information Processing Systems, Neural Information Processing Systems*.
- Shi, L.; Cao, L.; Wang, J.; and Chen, B. 2024. Enhanced Latent Multi-view Subspace Clustering. *IEEE Transactions on Circuits and Systems for Video Technology*.
- Stadler, M.; Charpentier, B.; Geisler, S.; Zügner, D.; and Günnemann, S. 2021. Graph Posterior Network: Bayesian Predictive Uncertainty for Node Classification. *Neural Information Processing Systems, Neural Information Processing Systems*.
- Sun, J.; Zhang, J.; Li, Q.; Yi, X.; Liang, Y.; and Zheng, Y. 2022. Predicting Citywide Crowd Flows in Irregular Regions Using Multi-View Graph Convolutional Networks. *IEEE Transactions on Knowledge and Data Engineering*, 2348–2359.
- Wang, F.; Liu, Y.; Liu, K.; Wang, Y.; Medya, S.; and Yu, P. S. 2024. Uncertainty in Graph Neural Networks: A Survey. *arXiv preprint arXiv:2403.07185*.

Wang, X.; Ji, H.; Shi, C.; Wang, B.; Ye, Y.; Cui, P.; and Yu, P. S. 2019. Heterogeneous Graph Attention Network. In *The World Wide Web Conference*.

Xu, C.; Si, J.; Guan, Z.; Zhao, W.; Wu, Y.; and Gao, X. 2024. Reliable Conflictive Multi-View Learning. *arXiv preprint arXiv:2402.16897*.

Yan, K.; Wen, J.; Xu, Y.; and Liu, B. 2020. Protein fold recognition based on auto-weighted multi-view graph embedding learning model. *IEEE/ACM Transactions on Computational Biology and Bioinformatics*, 18(6): 2682–2691.

Yang, Y.; Cui, H.; and Yang, C. 2023. Ptgb: Pre-train graph neural networks for brain network analysis. *arXiv preprint arXiv:2305.14376*.

Yao, K.; Liang, J.; Liang, J.; Li, M.; and Cao, F. 2022. Multi-view graph convolutional networks with attention mechanism. *Artificial Intelligence*, 307: 103708.

Yu, P.; Tan, Z.; Lu, G.; and Bao, B.-K. 2023. Multi-view graph convolutional network for multimedia recommendation. In *Proceedings of the 31st ACM International Conference on Multimedia*, 6576–6585.

Zhang, M.; Li, T.; Li, Y.; and Hui, P. 2020. Multi-View Joint Graph Representation Learning for Urban Region Embedding. In *Proceedings of the Twenty-Ninth International Joint Conference on Artificial Intelligence*.

Zhang, Q.; Wei, Y.; Han, Z.; Fu, H.; Peng, X.; Deng, C.; Hu, Q.; Xu, C.; Wen, J.; Hu, D.; et al. 2024. Multimodal fusion on low-quality data: A comprehensive survey. *arXiv preprint arXiv:2404.18947*.

Zhang, X.; Yang, Y.; Zhai, D.; Li, T.; Chu, J.; and Wang, H. 2021. Local2Global: Unsupervised multi-view deep graph representation learning with Nearest Neighbor Constraint. *Knowledge-Based Systems*, 231: 107439.

Zhao, X.; Dai, Q.; Wu, J.; Peng, H.; Liu, M.; Bai, X.; Tan, J.; Wang, S.; and Yu, P. S. 2023. Multi-View Tensor Graph Neural Networks Through Reinforced Aggregation. *IEEE Transactions on Knowledge and Data Engineering*, 35(4): 4077–4091.

Zhu, M.; Wang, X.; Shi, C.; Ji, H.; and Cui, P. 2021. Interpreting and unifying graph neural networks with an optimization framework. In *Proceedings of the Web Conference 2021*, 1215–1226.